Thermal shock experiments and inelastic calculations in piping systems

M.N.Berton & H.G.Failla
CEA-CEN Cadarache, DRNR/STRA, St-Paul-lez-Durance, France
P.Permezel
Electricité de France, SEPTEN, Villeurbanne

ABSTRACT

The VICTUS tests are sodium thermal shock experiments on LMFBR pipes to qualify computer codes and analysis procedures for structures and loadings of this type. The initial test results and calculations were presented at SMIRT 8 : a plane expansion loop with four elbows under in-plane bending loads was submitted to thermal shocks until shakedown occurred.

This paper covers the second test phase : a plane expansion loop under primary out-of-plane bending and torsion loads was subjected to thermal shocks until shakedown. The results confirm the observations recorded for the first expansion loop.

The test results are then compared with local calculations for torsion and ovalization. This study makes it possible to test certain plasticity models and their ability to account for thermal ratchetting.

1 THE "VICTUS" TESTS

1.1 Background Information

The entire test series was presented at SMIRT 8 together with the results obtained for the first test section (1). The same paper described the measurement, recording and data analysis procedures. Calculated results for expansion loop N° 1 were discussed and compared with the test findings in another paper (2).

1.2 Expansion loop N° 2

Figure 1 shows the geometrical characteristics of the second expansion loop, a 316L stainless steel element manufactured as described in (1).

The test specimen was subjected to the following loading :

- Primary stress out-of-plane loading was created by a counterweight at the top center of the loop (Figure 1). Both ends of the loop were clamped. This load alone was not sufficient to induce plastification, and created out-of-plane bending and torsion loading in both lower elbows.
- In this configuration the assembly was subjected to cold shocks resulting in a 130-150°C wall temperature gradient, without causing

significant impeded expansion. These shocks were repeated to shakedown.

- After shakedown to the cold shocks, the loop was subjected to a hot shock of the same amplitude.

2 TEST RESULTS WITH EXPANSION LOOP N°2

Although shakedown was observed after five cold shocks, a total of ten cycles were sustained without any further measurable distorsion. A new plastification was obtained, however, when the test specimen was submitted to a hot shock (thermal shock n° 11).

2.1 Residual Displacement at the Top of the Loop

Residual displacement measurements are used to determine whether shakedown has occured. The following values were measured for each thermal shock.

	Cold Shocks						Hot Shock
Thermal Shock N°	1	2	3	4	5	6	11
Max steel temp gradient °C	122	125	133	137	130	133	-126
Residual displacement mm	6.5	1.5	2.2	1.1	1.0	0	4.5
Cumulative residual displacement	6.5	8.0	10.2	11.3	11.4	11.4	15.9

Shocks 3 and 4 had the highest amplitude (cf steel temperature gradients); this no doubt accounts for the accident in the diminishing residual displacement observed after the successive cold shocks.

2.2 Temperatures and Displacements during the Thermal Shocks

Figures 2 (shock N° 1) and 3 (hot shock N° 11) show the displacements at the top of the loop during the thermal shock, the mean steel temperature and the equivalent linear temperature gradient. The last two values are calculated (thermal conduction calculation) from measured temperatures at the loop inlet and outlet.

2.3 Residual Ovalization

Plastification occurred primarily in the two lower elbows. The residual ovalization due to the first cold shock, the cumulative results for shocks 2 through 10 and the result for (hot) shock 11 are shown in figure 4. Ovalization was oriented about 45° from the loop plane, as could be expected under the test loading conditions (out-of-plane torsion and bending).

The mean and maximum ovalization (the incremental values due to each shock) recorded for the lower elbows are indicated in the following table.

Elbow	Thermal Shock	Mean Values		Maximum Values	
		Mean Ovalization	Mean Angle	Maximum Ovalization	Angle
C1	1	1.59 x 10-3	33°	2.64 x 10-3	32°
	2- 10*	0.78 x 10-3	48°	0.95 x 10-3	49°
	11	1.36 x 10-3	47°	2.44 x 10-3	31°
C4	1	1.06 x 10-3	-44	1.33 x 10-3	-44°
	2- 11*	2.38 x 10-3	-37°	3.68 x 10-3	-42°
* Cumulative Value					

2.4 Residual Torsion

Accurate residual torsion measurements are only available for shock N°1 and for the cumulative result of shocks 2 through 11. The following values were recorded for the lower horizontal straight portions :

Thermal Shock	Residual Torsion
1	0.8 x 10-6 rd/mm
2-11	1.2 x 10-6 rd/mm

2.5 Notes on the Test Results

These results for out-of-plane bending and torsion loads confirm the findings for expansion loop N°1 with planar bending loads :

- Deformation was noted in the primary loading direction (45° ovalization)
- The thermal ratchetting phenomenon confirms the contribution as a secondary loading of the thermally radial loading induced stresses through the wall thickness.

3 LOCAL PLASTIC CALCULATIONS : COMPARISON WITH EXPERIMENTAL MEASUREMENTS

Local shell calculations were performed in which primary stress loading was applied to a small portion of the expansion loop, and thermal shocks were then superimposed. These analyses were done to test various plasticity models before undertaking a full shell calculation as was done for the first test (2). Two zones of the expansion loop were selected for these calculations :

- a section of the lower horizontal straight portion submitted to torsional loading,
- a section of the lower elbow submitted to bending and induced ovalization loads.

The maximum thermal and mechanical load values are specified in figure 6. For the thermal loads, the values correspond to the test load referenced to a mean temperature of 0°C. This procedure was used to analyze six cold shocks followed by a hot shock.

3.1 Used Plasticity Models

Four plasticity models were investigated :
- isotropic model
- bilinear kinematic model
- trilinear kinematic model.

Figure 5 shows the monotonic curves of this three models

- A nonlinear kinematic model developed by J.L.Chaboche (4) was then applied. The principles of this model are briefly summarized here :

Notations :

ε_* cumulative plastic deformation
$\underset{\sim}{\sigma}$ stress tensor
$\underset{\sim}{\varepsilon}_p$ plastic deformation tensor
J Von Mises criterion
$\underset{\sim}{X}_k$ plasticity sphere translation tensors (kinematic variables)
R plasticity sphere radius (isotropic variable)
$\dot{}$ derivative with respect to

Equations defining the model :

plasticity law : $J_2(\underset{\sim}{\sigma} - \underset{\sim}{X}) - R(\varepsilon_*) = 0$

$$\dot{\underset{\sim}{X}}_k = C_k (2/3\, a_k \dot{\underset{\sim}{\varepsilon}}_p - \underset{\sim}{X}_k)$$

$$\dot{R} = B(R_m - R) \qquad R(0) = R_0$$

A number of models of this type with three, five and seven parameters (depending on the k value) were tested, with identification on cyclic tests and monotonic curves for this material, or using standard parameters for this grade of steel. The parameter selection was the first difficulty encountered in using this type of model.

Only two examples with three parameters representative of the results that can be obtained will be discussed here.

In the 3-parameter model, k = 1 (a single kinematic variable), and the radius of the plasticity sphere is constant $R = R_o$ (B = 0). The model is thus characterized by A,C and R (stress values in hbar) :

- Chaboche 1 A = 22.07 C = 1.77 x 10^3 Ro = 10
- Chaboche 2 A = 19.09 C = 1.077 x 10^3 Ro = 14

3.2 Torsion Analysis (lower horizontal straight portion)

The analysis covered a small section of the straight portion in axisymetrical coordinates with mode 0 (tangential) loading to simulate torsional loading, using the INCA of the CASTEM system (3).

One of the ends is clamped.The other end is rotation impeded in the plane containing the axis (pine continuity condition).

The analysis characteristics were the following : 1 thin shell element with 7 plasticity integration points in the shell thickness submitted to mode 0 loading to simulate the primary torsion load (moment corresponding to the force applied on the top of the expansion loop : cf figure 5) submitted to thermal shocks. This analysis accurately represents the phenomena occurring in the straight portion away from the elbow.

The results are shown in figures 7 and 8.

Figure 7 shows the residual torsion values calculated with the different models after each shock, together with the estimated residual torsion distribution for each shock based on the experimental measurements : the latter value is weighted proportionally to the

residual displacement at the top of the expansion loop. It may be seen that the first three models do not give thermal ratchetting. The value given by the fifth model ("Chaboche 2") is too low, while the fourth model gives an overestimated result (there is no limit to the plastification after the sixth shock).

Figure 8 shows the sear stress evolution for each load and unload to assess the results given by the different models. It may be seen that with relatively low shear stresses (1-2 hbar) significant torsional plastification can be obtained simply by superimposing thermal shocks.

3.3 Ovalization Analysis (most heavily loated section of the lower elbows : section where ovalization is the highest).

This analysis concerns an elbow section, using a thin shell cross section with 7 plasticity integration points in the shell thickness under generalized plane deformation (i.e. nonzero out-of-plane deformation but maintaining the cross section planar : see reference (5)). The calculation was performed using the INCA code, and the cross section was meshed with 48 shell elements.

Primary loading was simulated as follows :

- a beam-type moment resulting in bending perpendicular to the plane (possible in generalized plane deformation)
- internal pressure loading at sin $2\theta, 3\theta, 4\theta, 5\theta$. An elastic calculation with the TRICO shell code (CASTEM System) for the entire expansion loop gived us the circumferential stress repartition in the most loaded section. A Fourier series decomposition allows for the calculation of the pressure loading which produce the same circumferential stresses. Figure 9 compares the stresses as given by TRICO with our local INCA calculation.

The cold shocks and hot shock loading is then added (figure 6). The results are shown in figures 10, 11 and 12.

Figure 10 indicates the residual ovalization calculated with the different models after each shock, together with the estimated residual ovalization distribution for each shock, based on the test measurements and weighted proportionally to the residual displacement at the top of the expansion loop. The same observations may be made as for the previous analysis : the Chaboche model is the only one that gives thermal ratchetting. Plastification is not limited for the 5th shock with the "Chaboche 1" formulation, while "Chaboche 2" seems to provide more accurate results and also better accounts for the thermal shock (N° 11).

Figure 11 shows the circumferential strains on load and unload for the cold shocks. The "Chaboche" models tend to provide symmetrical stress values for load and unload.

Figure 12 shows the detailed cyclic loading with three different plasticily models : isotropic, kinematic, Chaboche 1. The isotropic model produces elastic shakedown and the kinematic one plastic shakedown

4 CONCLUSION

The tests on the N° 2 expansion loop confirm the results observed on the first expansion loop : thermal ratchetting in the direction of the primary loading developed under the effect of repeated thermal

shocks. It is thus important to take into account the $\Delta T1$ temperature gradient in the wall thickness when analyzing this phenomenon.

Local calculation with various plasticity models demonstrated the superiority of the nonlinear kinematic model developed by M. Chaboche, although the thermal ratchetting is overestimated and the parameter values are relatively difficult to determine. Overall shell calculations for the complete expansion loop are planned.

The test program will proceed with a third 3-dimensional expansion loop test in which the primary loading will be replaced by impeded expansion loading.

REFERENCES

(1) M.N. Berton, J.L. Carbonnier and P. Permezel. Thermal Shock Experiments in Piping Systems. E 6/4, SMIRT 8, 1985.

(2) M.N. Berton and P. Permezel. Piping System Inelastic Calculation during Thermal Shocks : Comparison with Experiments. E 6/5, SMIRT 8, 1985.

(3) A. Hoffmann and A. Combescure. CASTEM (CEASEMT) : A System of Finite Element Computer Programs. Paper 40,Porto Alegre, Brazil,1978.

(4) J.L. Chaboche, K. Dang Van and G. Cordier. Modelization of the Strain Memory Effect on the Cyclic Hardening of 316 Stainless Steel. - L 11/3, SMIRT 5, 1979.

(5) Generalized Plane Strains : An Interesting and Efficient Extension of the Standard Plane Stress and Plane Strain Analysis. A.Combescure B.8.8. SMIRT 8, 1985.

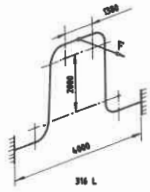

LOADING :
F = 1200 daN ΔT = 130-150°C
PIPES DIMENSIONS :
Diameter Φ = 219.18 mm
Thickness e = 8.18 mm
Bend's radius R = 305 mm

FIGURE 1 : VICTUS - TEST SECTION 2

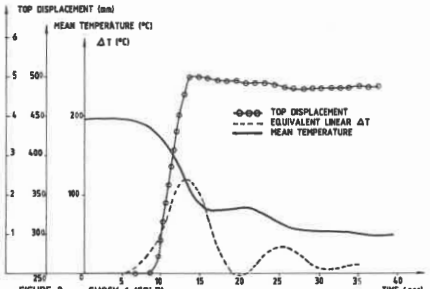

FIGURE 2 : SHOCK 1 (COLD)
DISPLACEMENT DURING THE SHOCK
EQUIVALENT LINEAR THERMAL GRADIENT AND MEAN TEMPERATURE

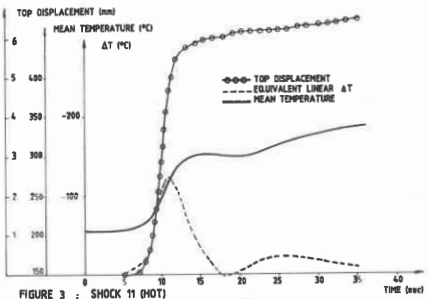

FIGURE 3 : SHOCK 11 (HOT)
DISPLACEMENT DURING THE SHOCK
EQUIVALENT LINEAR THERMAL GRADIENT AND MEAN TEMPERATURE

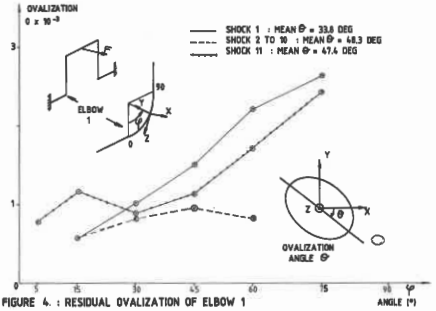

FIGURE 4. : RESIDUAL OVALIZATION OF ELBOW 1

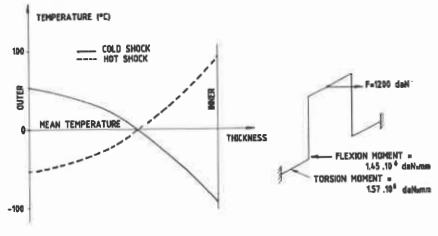

FIGURE 5 : LOADING :
TEMPERATURE REPARTITION IN THICKNESS
AND PRIMARY LOADING

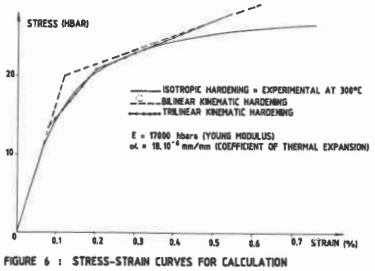

FIGURE 6 : STRESS-STRAIN CURVES FOR CALCULATION

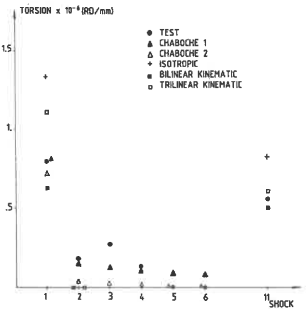

FIGURE 7 : RESIDUAL TORSION IN THE LOW STRAIGHT PART AFTER EACH SHOCK
TEST CALCULATION COMPARISON

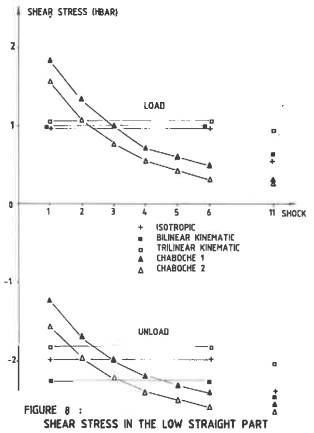

FIGURE 8 :
SHEAR STRESS IN THE LOW STRAIGHT PART

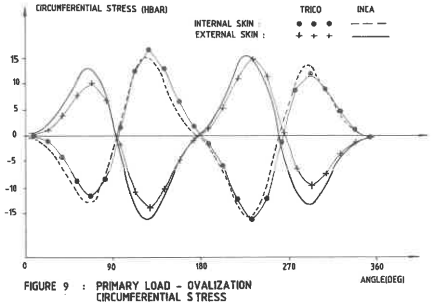

FIGURE 9 : PRIMARY LOAD - OVALIZATION
CIRCUMFERENTIAL STRESS

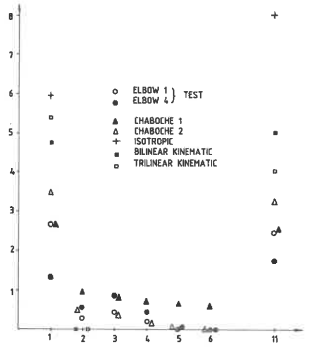

FIGURE 10 : RESIDUAL OVALIZATION IN THE LOW ELBOWS AFTER EACH SHOCK
TEST CALCULATION COMPARISON

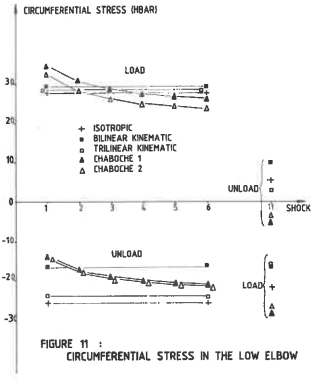

FIGURE 11 :
CIRCUMFERENTIAL STRESS IN THE LOW ELBOW

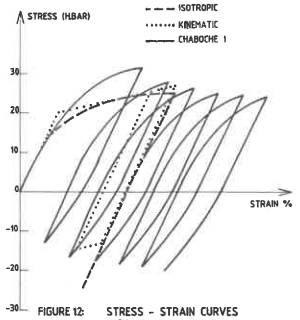

FIGURE 12: STRESS - STRAIN CURVES WITH DIFFERENT PLASTICITY MODELS
LOW ELBOW CALCULATION